

The Aspen–Amsterdam Void Finder Comparison Project

Jörg M. Colberg^{1,2}, Frazer Pearce³, Caroline Foster^{4,5}, Erwin Platen⁶,
Riccardo Brunino³, Mark Neyrinck⁷, Spyros Basilakos⁸, Anthony Fairall⁹,
Hume Feldman¹⁰, Stefan Gottlöber¹¹, Oliver Hahn¹², Fiona Hoyle¹³,
Volker Müller¹¹, Lorne Nelson⁴, Manolis Plionis^{14,15}, Cristiano Porciani¹²,
Sergei Shandarin¹⁰, Michael S. Vogeley¹⁶, Rien van de Weygaert⁶

¹ Carnegie–Mellon University, 5000 Forbes Ave, Pittsburgh, PA 15213, USA

² Astronomy Department, University of Massachusetts, Amherst, MA 01003, USA

³ School of Physics & Astronomy, University of Nottingham, Nottingham, NG7 2LE, UK

⁴ Bishop’s University, Department of Physics, 2600 College Street, Sherbrooke, QC J1M 0C8, Canada

⁵ Centre for Astrophysics & Supercomputing, Swinburne University of Technology, Hawthorn VIC 3122, Australia

⁶ Kapteyn Institute, University of Groningen, PO Box 800, 9700 AV Groningen, The Netherlands

⁷ Institute for Astronomy, University of Hawaii, Honolulu, HI 96822, USA

⁸ Research Center for Astronomy & Applied Mathematics, Academy of Athens, Soranou Efessiou 4, 11-527, Athens, Greece

⁹ Department of Astronomy, University of Cape Town, Private Bag, Rondebosch 7700, South Africa

¹⁰ Department of Physics and Astronomy, University of Kansas, Lawrence, KS 66045, USA

¹¹ Astrophysikalisches Institut Potsdam, An der Sternwarte 16, 14482 Potsdam, Germany

¹² ETH Zürich, 8093 Zürich, Switzerland

¹³ Department of Physics and Astronomy, Widener University, One University Place, Chester, PA 19013

¹⁴ Institute of Astronomy & Astrophysics, National Observatory of Athens, I. Metaxa & B. Pavlou, P. Penteli 152 36, Athens, Greece

¹⁵ Instituto Nacional de Astrofisica, Optica y Electronica (INAOE) Apartado Postal 51 y 216, 72000 Puebla, Pue., Mexico

¹⁶ Department of Physics, Drexel University, 3141 Chestnut Street, Philadelphia, PA 19104, USA

Accepted 200? ???? ?. Received 2007 ???? ??. in original form 2007 xx

ABSTRACT

Despite a history that dates back at least a quarter of a century studies of voids in the large–scale structure of the Universe are bedevilled by a major problem: there exist a large number of quite different void–finding algorithms, a fact that has so far got in the way of groups comparing their results without worrying about whether such a comparison in fact makes sense. Because of the recent increased interest in voids, both in very large galaxy surveys and in detailed simulations of cosmic structure formation, this situation is very unfortunate. We here present the first systematic comparison study of thirteen different void finders constructed using particles, haloes, and semi–analytical model galaxies extracted from a subvolume of the Millennium simulation. The study includes many groups that have studied voids over the past decade. We show their results and discuss their differences and agreements. As it turns out, the basic results of the various methods agree very well with each other in that they all locate a major void near the centre of our volume. Voids have very underdense centres, reaching below 10 percent of the mean cosmic density. In addition, those void finders that allow for void galaxies show that those galaxies follow similar trends. For example, the overdensity of void galaxies brighter than $m_B = -20$ is found to be smaller than about -0.8 by all our void finding algorithms.

Key words: cosmology: theory, methods: N-body simulations, dark matter, large-scale structure of Universe

1 INTRODUCTION

Large regions of space that are only sparsely populated with galaxies, so-called voids, have been known as a feature of

galaxy surveys since the first of those surveys was compiled, the most well-known cases being the famous void in Boötes, discovered by Kirshner et al. (1981), and the first void sam-

ple of de Lapparent, Geller & Huchra (1986). However, due to the fact that voids occupy a large fraction of space, only recently have galaxy surveys become large enough to allow systematic studies of voids and the galaxies inside them. For recent studies of voids and void galaxies in the two-degree field Galaxy Survey (2dFGRS, Colless et al. 2001) and the Sloan Digital Sky Survey (SDSS, York et al. 2000) see Hoyle & Vogeley (2004), Ceccarelli et al. (2006), Patiri et al. (2006a), Tikhonov (2006), von Benda-Beckmann & Müller (2008) and Rojas et al. (2004), Goldberg et al. (2005), Hoyle et al. (2005), Rojas et al. (2005), Patiri et al. (2006b), respectively. Also see Croton et al. (2004) for a recent, detailed study of the void probability function in the 2dF.

On the theoretical side, progress has been mirrored by vast improvements in models and simulations, with systematic studies of large numbers of voids now being common (see, for example, the early works by Regos & Geller 1991, Dubinski et al. 1993 or Van de Weygaert & Van Kampen 1993, and the more recent Arbabi-Bidgoli & Müller 2002, Mathis & White 2002, Benson et al. 2003, Gottlöber et al. 2003, Goldberg & Vogeley 2004, Sheth & Van de Weygaert 2004, Bolejko et al. 2005, Colberg et al. 2005, Padilla et al. 2005, Brunino et al. 2006, Furlanetto & Piran 2006, Hoefl et al. 2006, Lee & Park 2006, Park & Lee 2006, Patiri et al. 2006c, Shandarin et al. 2006). Theory shows that voids are a real feature of large-scale structure, since initially underdense regions grow in size as overdense regions collapse under their own gravity (see, for example, Sheth & Van de Weygaert 2004). But while the general picture appears to be well supported by the standard Λ Cold Dark Matter (Λ CDM) cosmology, Peebles (2001) pointed out some potentially critical issues. Does the Λ CDM cosmology produce too many objects in voids that have no observational counterparts? A detailed discussion of other reasons why studies of voids are an interesting topic is beyond the scope of this paper. Briefly, their role as a prominent feature of the Megaparsec Universe means that a proper and full understanding of the formation and dynamics of the Cosmic Web is not possible without probing the structure and evolution of voids. A second rationale is that of inferring global cosmological information from the structure and geometry of and outflow from voids. The third aspect is that of providing a unique and still largely pristine environment for testing theories of the formation and evolution of galaxies.

Despite the growing interest in voids and the large number of recent studies, a fairly significant problem remains: as it turns out, almost every study uses its own void finder. There is general agreement that there are voids in the data or in the simulations, but many different ways were proposed to find them. Thus, the resulting voids are either spherical (with or without overlap), shaped like lumpy potatoes¹, or they percolate all across the studied volume. What is more, some groups do not allow for the existence of void galaxies, whereas many others do. An added complication is that many theoretical studies use the dark matter distribution to find voids, whereas observational studies have to rely on galaxies. As a consequence, it is not clear how the results from studies done by different groups can be compared, es-

pecially if observational and theoretical results are brought together. What most studies so far can agree on is that a) voids are very underdense in their centres (approaching around five percent of the mean density) and that b) voids often have very steep edges. In other words, the number of both observed and simulated galaxies increases very rapidly when reaching the edge of a void, and the corresponding result has been found for the density of dark matter in studies that used dark-matter only simulations.

Given the disagreements in the different methods, which are in part due to the different nature of the data sets used, the aim of this work is very modest. We apply thirteen different void finders, all of which have been used over the past decade to study voids, to the same data set in order to compare the results. As our data set we use particles, haloes, and semi-analytical model galaxies (Croton et al. 2005) from a subvolume of the Millennium simulation (Springel et al. 2005) specifically selected to be underdense and therefore void-rich. That way, while the methods are as different as finding connected cells on a density grid and identifying empty regions in the model galaxy distribution by eye, a meaningful comparison is still possible, since each void finder treats a subset of the same data set.

The aim of this paper is *not* to argue which void finder provides the best way to identify voids. We do hope, however, that this paper will allow the reader to understand the differences between the different void finders so that it will be easier to compare different studies of voids in the literature. We also hope that this paper will trigger more detailed follow-up studies to work towards a more unified view of this topic and to study properties of voids not covered here, such as for example their shapes and orientations, in detail.

This paper is organised as follows: in Section 2 we detail the simulation from which the test region was extracted and describe the procedure each group was asked to undertake. In Section 3 we briefly describe each void finding algorithm, before we undertake a comparison of the voids found in Section 4. Section 5 contains a summary and conclusions.

2 THE SIMULATION AND EXTRACTION PROCEDURE

For this work, we use the Millennium simulation (Springel et al. 2005) and a matched $z = 0$ galaxy catalogue, created using a semi-analytical galaxy formation model (Croton et al. 2005). The simulation of the concordance Λ CDM cosmology contains 2160^3 particles in a (periodic) box of size $500 h^{-1}$ Mpc in each dimension. The cosmological parameters are total matter density $\Omega_m = 0.25$, dark energy/cosmological constant $\Omega_\Lambda = 0.75$, Hubble constant $h = 0.73$, and the normalisation of the power spectrum $\sigma_8 = 0.9$. With these parameters, each dark matter particle has a mass of $8.6 \times 10^8 h^{-1} M_\odot$.

In the Millennium simulation volume we located a $60 h^{-1}$ Mpc region centred on a large void and extracted the coordinates of the 12,528,667 dark matter particles contained within it. This subvolume thus has a mean density which is lower than the cosmic mean, corresponding to an overdensity $\delta = \rho/\bar{\rho} - 1 = -0.28$.

We also extracted a list of the 17,604 galaxies together with their BVR_{IK} dust corrected magnitudes (down to B=

¹ JMC admits that this picture, while being accurate, is not very pretty.

10) that are present in the semianalytic catalogue of Croton et al. (2005) within this volume and the 4,006 dark matter halos present in the subfind catalogue (a clean spherical overdensity based catalogue) with masses greater than $10^{11} h^{-1} M_{\odot}$. Note that while the small volume prohibits statistical comparisons between void finders it allows for void-by-void comparisons.

Each group was asked to run their void finder with their preferred parameters on this database and return a void list for the voids found, tagging each of the dark matter particles, galaxies, and haloes with the void identifier of the void they resided in. This allowed simple plotting and analysis of each void sample. For overlapping voids, the dark matter particle was to be assigned to the larger void. As the region is not periodic we only requested information about voids whose centres lay within the central $40 h^{-1}$ Mpc region (i.e. the outer $10 h^{-1}$ Mpc was to be neglected).

The top left and top centre panels of Figure 1 show slices of thickness $5 h^{-1}$ Mpc through this central region. The top left panel only contains the distribution of the dark matter, whereas the top centre panel includes model galaxies on top of the dark matter distribution. The largest halo has a mass of only $1.75 \times 10^{12} h^{-1} M_{\odot}$, so filaments in these images correspond only to the less massive filaments in standard slices through the dark matter distribution as seen in, for example, Springel et al. (2005). Furthermore, the slice contains a total of 145,194 dark matter particles, equivalent to an overdensity of $\delta = -0.77$. It is important to keep these numbers in mind when studying the results obtained by the various void finders. Subsequent panels show the largest void identified by each group and those galaxies contained within all voids identified.

3 VOID FINDERS

This section gives a brief outline of the void finders used for this study, grouped into those which rely on the dark matter distribution and those which rely on the sparser galaxy or halo distributions (also see Table 1 for a general overview). For more details, the interested reader is referred to the individual studies by the different groups. Anyone simply interested in the results can skip to the next section. Please note that in this study, all group finders use real-space data.

3.1 Finders based on the dark matter distribution

3.1.1 Colberg: Irregularly shaped underdense regions around local density minima

This method was introduced in Colberg et al. (2005), where it was used to study voids in the dark matter distribution of a suite of large N-body simulations. The starting point for Colberg et al.'s void finder is the adaptively smoothed distribution of the full dark matter distribution in a simulation. Proto-voids are constructed in a fashion quite similar to Hoyle & Vogeley's void finder, the difference being that Colberg's uses local minima in the density field as the centres of voids, and the mean density of the spherical proto-voids is required to be smaller or equal to an input threshold, which, following a simple linear theory argument, is taken to be $\delta = -0.8$ (Blumenthal et al. 1992). Proto-voids are

then merged according to a set of criteria, which allow for the construction of voids that can have any shape, as long as two large regions are not connected by a thin tunnel (which would make the final void look like a dumbbell). The voids thus can have arbitrary shapes, but they typically look like lumpy potatoes.

For this study, a grid of size 480^3 and a minimum void radius of $r_{\min} = 2.0 h^{-1}$ Mpc were used. In the following, this void finder and its results are referred to as *Colberg*.

3.1.2 Pearce: Spheres around local density minima

For every particle in the Millennium simulation local densities were calculated by smoothing over the nearest 32 neighbours using a beta spline kernel (Monaghan & Lattanzio 1985). This list was then ranked in density order (starting from the most underdense particle), and independent initial void centres were chosen such that they were more than $2 h^{-1}$ Mpc away from a previously selected centre (up to $\delta = -0.965$). The radial distribution of particles about these trial centres was then used to calculate the first up-crossing above $\delta = -0.9$. These radii were then sorted in size order, and the resulting list was cleaned by removing voids whose centre lay within an already found void. The 3,024 voids found by this procedure were used as the starting points for the more traditional halo based group finder used by Brunino et al. (2007). In the following, this void finder and its results are referred to as *Pearce*.

3.1.3 Hahn/Porciani: Equation of motion in smoothed density field

A stability criterion for test-particle orbits is used to discriminate four environments with different dynamics (Hahn et al. 2006). The classification scheme is based on a series expansion of the equation of motion for a test particle in the smoothed matter distribution. The series expansion yields a zero order term, the acceleration, and a second order term, the tidal field T_{ij} (Hessian of the potential). The eigenvalues of T_{ij} characterise the triaxial deformation of an infinitesimal sphere due to the gravitational forces. Voids are classified as those regions of space where T_{ij} has no positive eigenvalues (tidally unstable).

The method has one free parameter, the size of the Gaussian filter used to smooth the potential. This parameter is set to $R_s = 2.09 h^{-1}$ Mpc, which corresponds to a mass of $10^{13} h^{-1} M_{\odot}$ contained in the filter at mean density. This choice gives excellent agreement with a visual classification (see the discussion in Hahn et al. 2006). This mass scale corresponds to about $2 M_*$ at $z = 0$.

The tidal field eigenvalues are evaluated on a grid. Then, contiguous regions classified as voids are linked together. Voids can thus have arbitrary shapes, and their volumes are proportional to the number of cells linked together. In the following, this void finder and its results are referred to as *Hahn/Porciani*.

Author	Base	Method
Brunino	Halo	Spherical regions in halo distribution
Colberg	Dark matter density field	Irregularly shaped underdense regions around local density minima
Fairall	Galaxies	Empty regions in galaxy distribution
Foster/Nelson	Galaxies	Empty regions in galaxy distribution
Gottlöber	Halo/Galaxies	Spherical empty regions in point set
Hahn/Porciani	Dark matter density field	Tidal instability in smoothed density field
Hoyle/Vogele	Galaxies	Empty regions in galaxy distribution
Müller	Halo/Galaxies	Empty convex regions in point set
Neyrinck	Dark matter density field	ZOBOV, depressions in unsmoothed DM field
Pearce	Dark matter	Local density minima spheres
Platen/Weygaert	Dark matter density field	Watershed DTFE
Plionis/Basilakos	Dark matter density field	Connected underdense density grid cells
Shandarin/Feldman	Dark matter density field	Connected underdense density grid cells

Table 1. An overview of the void finders used in this study.

3.1.4 Neyrinck: ZOBOV

ZOBOV (ZOnes Bordering On Voidness, Neyrinck (2008)) is an inversion of a publicly available halo-finder, VOBOZ² (Neyrinck et al. 2005). ZOBOV differs from VOBOZ in that ZOBOV looks for density minima instead of maxima, and does not consider gravitational binding. ZOBOV has some unique features: it is entirely parameter-free, working directly on the unsmoothed particle distribution; and, it returns all (even possibly spurious) depressions surrounding density minima, along with estimates of the probability that each arises from Poisson noise.

The first step is density estimation and neighbour identification for each dark-matter particle, using what Schaap (2007) calls the Voronoi Tessellation Field Estimator. ZOBOV then partitions the particles into zones (depressions) around each minimum. Each particle jumps to its lowest-density neighbour, repeating until it reaches a minimum. A minimum’s *zone* is the set of particles which flow downward into it. Zones resemble voids, but because of unsmoothed discreteness noise, many zones are spurious, and others are only cores of voids detected by eye. So, ZOBOV must join some zones together to form voids. Voids around each zone grow by analogy with a flooding landscape (representing the density field): water flows into neighbouring zones, adding them to the original zone’s void. The zone’s void stops growing when the water spills into a zone deeper than the original zone, or the whole field is submerged. The probability that a void is real is judged by the ratio of the density at which this happens to the void’s minimum density.

This density contrast r is converted to a probability through comparison with a Poisson point distribution; see Neyrinck et al. (2005) for details. The ZOBOV catalogue used for comparison with other void-finders includes only voids exceeding a $5\text{-}\sigma$ probability threshold, which corresponds to a density contrast of 2.89. Also, subvoids exceeding this threshold have been removed from parent voids. In the following, this void finder and its results are referred to as *Neyrinck*.

3.1.5 Platen/Weygaert: Watershed void finder

The Watershed Void Finder (WVF) is an implementation of the Watershed Transform (WST) for image segmentation towards the analysis of the Cosmic Web. The Watershed Transform is a familiar concept in mathematical morphology and was first introduced by Beucher & Lantuejoul (1979, also see Beucher & Meyer 1993).

The WST delineates the boundaries of separate domains, ie. the *basins*, into which which the yields of e.g. rainfall will collect. The analogy with the cosmological context is straightforward: *voids* are to be identified with the *basins*, while the *filaments* and *walls* of the cosmic web are the ridges separating the voids from each other.

The voids are computed by an algorithm that mimics the flooding process. First the cosmological point distribution is transformed by the DTFE technique into a density field. DTFE (Schaap & van de Weygaert 2000, Schaap 2007) assures an optimal rendering of the hierarchical, anisotropic and voidlike nature and aspects of the weblike cosmic matter distribution. The density field is adaptively smoothed by *nearest neighbour median filtering* (Platen et al. 2007). Minima are selected from the smoothed field and marked as the sources of flooding. While the “watershed” level rises a growing fraction of the “landscape” will be flood: the basins expand. Ultimately basins will meet at the ridges, saddle-points in the density field. These ridges define their boundaries, and are marked as edge separating the two basins. The procedure is continued until the density field is completely immersed, leaving a division of the landscape into individual segments separated by *edges*. The edges delineate the skeleton of the field and outline the *voids* in the density field.

The voids in the watershed procedure have no shape constraints. By definition the voids fill space completely. Nearly without exception galaxies and dark halos are located on the ridges of the cosmic web, implying a minimal amount of galaxies to be located in the watershed void segments.

² Available at <http://ifa.hawaii.edu/~neyrinck/VOBOZ>.

3.1.6 *Plionis/Basilakos: Connected underdense density grid cells*

This void finder is applied on a regular 3-D grid of the DM particle distribution or of a smoothed galaxy distribution, and it is based in identifying those grid cells (which we call “void cells”) whose density contrast lies below a specific threshold. Then all neighbouring (touching) “void cells” are connected to form candidate voids (see also Plionis & Basilakos 2002). Therefore, by construction, voids do not overlap, and they can have an arbitrary shape, which is approximated by an ellipsoidal configuration (see Plionis & Basilakos 2002). Of course, increasing the threshold one tends to percolate through the available volume by connecting voids. The threshold below which the “void cells” are identified is chosen so that a specific fraction of the probability density function (pdf) is used. For example, the voids presented here are based on the lowest 12.5% density “void cells”, which corresponds to $\delta\rho/\rho \simeq -0.92$.

In order to identify significant voids from our candidate list we compare with voids found in 1000 realizations of the DM particle distribution, using again the lowest 12.5% density void cells of each “random–realization” pdf. Now a probability curve as a function of void size can be built. Smaller voids appear with a large frequency in the random realizations and thus a candidate void is considered as significant only if its probability of appearing in a random distribution is < 0.05 .

There are two free parameters in this void identification procedure: (a) The grid cell size and (b) the threshold below which void cells are identified. The first is selected arbitrarily in this work such that it roughly encloses the volume of a typical cluster of galaxies, $(2\text{Mpc})^3$, while the second is selected such that it maximises the number of significant voids. In the following, this void finder and its results are referred to as *Plionis/Basilakos*.

3.1.7 *Shandarin/Feldman: Connected underdense density grid cells*

Voids are defined as the individual 3D regions of the low-density excursion set fully enclosed with the isodensity surfaces (for more details see Shandarin et al. 2006). Here, we first generate the density field on a uniform rectangular grid using the cloud-in-cell (CIC) technique. The grid parameter is chosen to be equal to the mean separation of particles in the whole simulation $d = (500/2160)h^{-1}$ Mpc. The CIC algorithm uses particles of the same size. Then the density field is smoothed with a spherical Gaussian filter with $R_G = 1h^{-1}$ Mpc, assuming nonperiodic boundary conditions and empty space beyond the boundaries. In the analysis we use only the central part of the cube, slicing $4.5d$ from every face of the initial cube affected by smoothing. The final cube consists of 250^3 grid sites with the volume of about 91% of the initial cube. Nonpercolating voids reach maximum sizes at the percolation transition (Shandarin et al. 2004). The technique makes no assumptions about the shapes of voids that generally are highly nonspherical. At higher thresholds the total volume in all but the percolating void drops off precipitously and the excursion set practically becomes a single percolating void. Our voids are identified at the percolation threshold $\delta \approx -0.88$ (filling fraction of

the voids, $\text{FF}_V = 20\%$). We find 19 voids larger than $5h^{-3}$ Mpc³. The largest void is of irregular shape and its volume is $V = 2.1 \times 10^4 h^{-3}$ Mpc³. There are neither halos nor galaxies inside these voids. Galaxies start to appear in the percolating void at $\delta > -0.86$ ($\text{FF}_V > 27\%$) and halos at $\delta > -0.63$ ($\text{FF}_V > 66\%$). In the following, this void finder and its results are referred to as *Shandarin/Feldman*.

3.2 Finders based on the galaxy or halo distribution

3.2.1 *Brunino: Spherical voids in halo catalogue*

This void finder algorithm uses the void centres provided by *Pearce’s* algorithm as an initial guess for the location of the underdense regions. These positions are then used to search for the maximum spheres that are empty of haloes with masses larger than $8.6 \times 10^{11} h^{-1} M_\odot$, or 1000 particles. To characterise the final position of the void centres and their radii we populate a sphere of radius $R = 5h^{-1}$ Mpc, centred on each initial position, with 2000 random points (the choice of these quantities has proved to be the most convenient in order to obtain a stable result). For every point in this sphere, the position of the closest four haloes lying in geometrically “independent” octants is found. The sphere defined by these four haloes is then built. This is repeated for all the 2000 random points. As a characterisation (position and radius) of the void, the biggest empty spherical region generated in the previous step is chosen.

It is important to stress that the position of the void defined in this way normally does not match the position of the initial guess. Furthermore, in the present work, voids whose centre turned out to lie inside a larger void have been discarded. A total of six void regions have been found in the volume of interest, three of which have been neglected applying this criteria. This algorithm is a variant of the one described in Patiri et al. (2006a) which has been developed to resemble the observational technique used to detect voids to enable a more direct comparison with simulations (e.g. Trujillo et al. 2006, Brunino et al. 2007) In the following, this void finder and its results are referred to as *Brunino*.

3.2.2 *Fairall: Voids in the galaxy distribution*

Voids have been located manually by inspection of slice visualisations: A moving slice, in x and y with thickness $\Delta z = 5h^{-1}$ Mpc, has been passed through the data in steps of $2.5h^{-1}$ Mpc. Its progress has been visualised by software that shows both individual galaxies and large-scale structures, the latter based on minimal spanning trees with percolations of $1h^{-1}$ Mpc or less (effectively “friends of friends”). The voids are conspicuous cavities, approximately spherical, empty or almost empty of galaxies, visible in consecutive slices, with sharply defined walls formed by large-scale structures. Since the voids interconnect with one another, the large-scale structures do not necessarily completely enclose each void. If a void departs from sphericity, an average radius is estimated. Where the data allow, distinct voids as small as $2.5h^{-1}$ Mpc (radius) are identified. In the following, this void finder and its results are referred to as *Fairall*.

3.2.3 *Foster/Nelson: Voids in the galaxy distribution*

The identification of voids is calculated using a prescription similar to that of Hoyle and Vogeley (2002). The algorithm has been extensively employed to analyse void structure and distribution using the results from the recently published Data Release 5 (DR5) of the Sloan Digital Sky Survey (SDSS) (see, Foster and Nelson 2007). The average distance to the third nearest neighbour (d) in the sample and its standard deviation (σ) are calculated. In order to ensure a high degree of confidence in identifying bona fide voids, we use the parameter $R_3 = d + \lambda \sigma$ to distinguish wall galaxies from field galaxies and set $\lambda = 2$. Wall galaxies are defined as those galaxies whose third nearest neighbour is closer than R_3 . All other galaxies are field galaxies. The wall galaxies are placed in a grid whose basic cell geometry is cubic having a side of length $R_3/2$. The empty cells are then identified and each empty cell acts as a seed from which holes are grown. A hole is defined as a sphere that is entirely devoid of wall galaxies. Its radius and centre are computed such that there are exactly 3 wall galaxies on its surface. Voids are then formed by amalgamating the overlapping holes starting with the largest holes. Only holes whose radius exceeds a certain threshold value ($R_{min} = 7.5 h^{-1}$ Mpc for this analysis) can form voids; those that are smaller are used to map out the boundary surface of a pre-existing void. Thus if there are no holes whose size exceeds the threshold, no voids will be identified. The position of the centre of each void is calculated by finding the ‘‘centre of volume’’. The position of the centre and the volume are calculated using Monte Carlo methods and the equivalent spherical radius is determined. In the following, this void finder and its results are referred to as *Foster/Nelson*.

3.2.4 *Gottlöber: Empty spheres in point set*

The void finder starts with a selection of point-like objects in three-dimensional space. These objects can be halos above some mass (or circular velocity) or galaxies above some luminosity. Thus voids are characterised by the threshold mass or luminosity.

For the data used here, $N_g = 380$ grid cells in each dimension were used, which corresponds to a grid cell size of $158 h^{-1}$ kpc. On this grid the point is found, which has the largest distance to the set of points defined above. This grid point is the centre of the largest void. This void is then excluded, and the procedure is repeated by searching for a point with the largest distance to the set. Iterating this procedure thus yields the full sample of voids

In principle, the algorithm allows to have a certain number of points (objects above the threshold mass or luminosity) inside the void. Here, this number is set to zero, i.e. the voids are completely empty with respect to the defined sample. Of course, they may contain objects with smaller masses or lower luminosities than the assumed threshold.

In principle, the algorithm allows for the construction of voids with arbitrary shape. The starting point is the spherical void described above. It can be extended by spheres of lower radius which grow from the surface of the void into all possible directions. However, in this test case this feature was switched off, and the search was restricted to spherical voids to avoid ambiguities of the definition of allowed devia-

tions from spherical shape. In the following, this void finder and its results are referred to as *Gottlöber*.

3.2.5 *Hoyle/Vogeley: Voidfinder*

Voidfinder was introduced in Hoyle & Vogeley (2002; *HV02*) and has been used frequently to locate voids in galaxy surveys (Hoyle & Vogeley 2004, Hoyle et al. 2005). Full details of how *voidfinder* works can be found in Hoyle & Vogeley (2002), so here we will only briefly summarise the algorithm. *Voidfinder* operates on samples of galaxies and is based on the ideas discussed in El-Ad & Piran (1997) and El-Ad et al. (1997). In a volume-limited galaxy catalogue (with a typical limit just fainter than M^*), galaxies are first pre-categorised into wall or void galaxies, depending on the distances to the galaxies’ third-nearest neighbours. Wall galaxies are then binned into cells of a cubic grid. Around the centres of all empty grid cells the largest possible spheres that are also empty are found. Finally, the set of unique voids is constructed by determining maximal spheres and their overlaps. *voidfinder* voids are non-spherical. A minimum void size of $10 h^{-1}$ Mpc is set to only select the largest, statistically most significant voids. For tests of *voidfinder* using simulation data see Benson et al. (2003). In the following, this void finder and its results are referred to as *Hoyle/Vogeley*.

3.2.6 *Müller: Empty convex regions in point set*

This grid based void finder looks first for empty base voids in the halo/galaxy sample, and then it adds extensions to approximate spherical voids. It was run first with only a base void search and then with extensions. The idea of the void finder is to look for empty nearly convex regions in the galaxy distribution. It is based on a grid on the survey volume where cells with galaxies are marked as occupied. In the next step, it looks for maximum cubes on the grid that are empty of galaxies and previously found voids. We call this a base voids, and get a first catalogue of cube voids, the most simple algorithm, but it produces a void catalogue with similar sizes as assuming a spherical base volume. A slightly more refined method is to extend the base voids along the faces with adding square sheets empty of galaxies and not contained in previously found voids. This extension procedure is iterated. To avoid extended fingers or bridges between voids, we require the extension to have a surface bigger than $2/3$ (an arbitrary parameter) of the previous one. These extended voids have on average the same volume in the extensions as in the base voids. We measure the size by the effective cube size, i.e. a cube of the same volume as the base plus extensions. Such voids are in general larger than selecting square voids. This void finder is based on the prescription of Kauffmann & Fairall (1991), which was further developed and tested by Müller et al. (2000) and Arbabi-Bidgoli & Müller (2002). It uses a 300^3 grid and includes voids with a minimum effective radius of $3 h^{-1}$ Mpc. In the following, this void finder and its results are referred to as *Müller*.

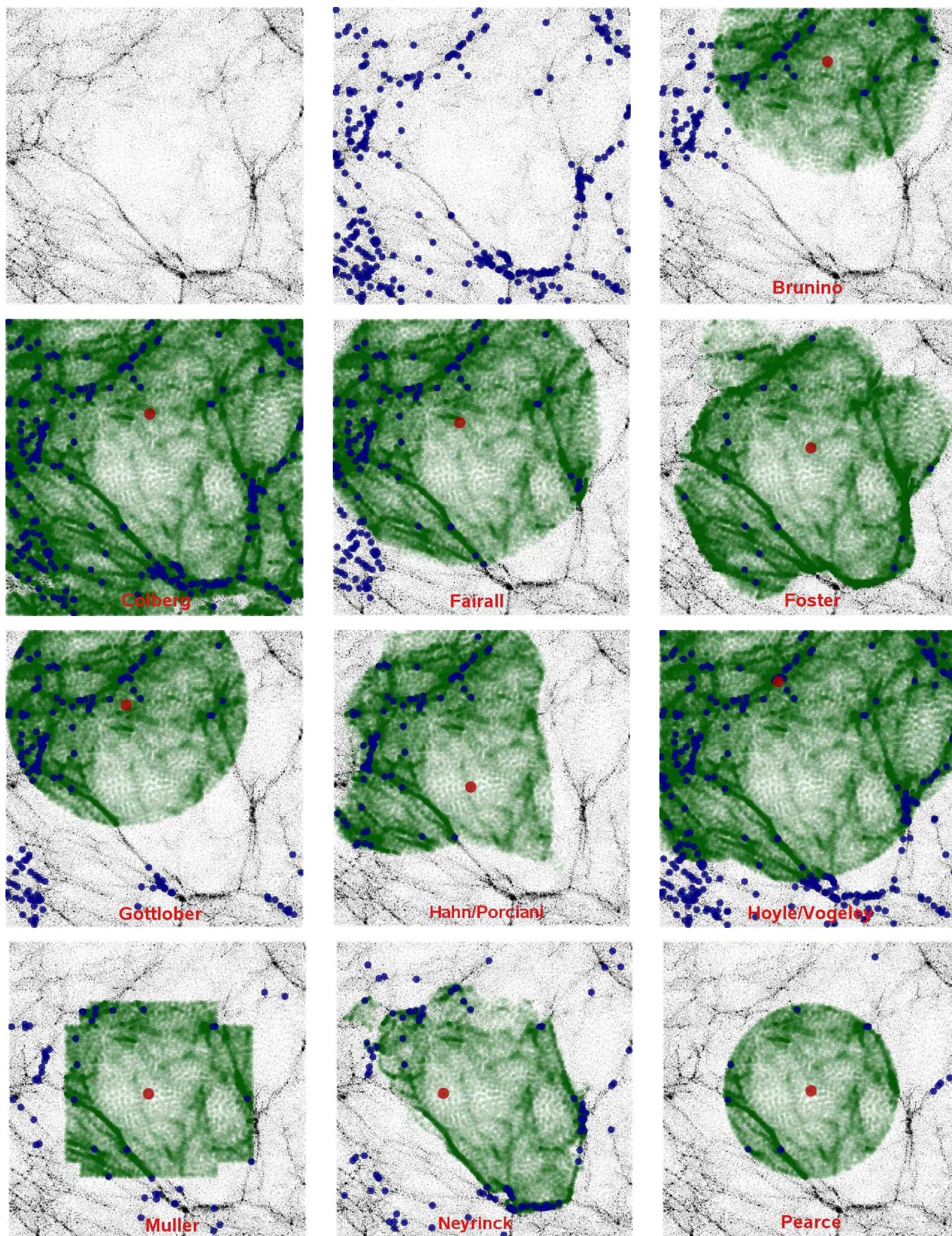


Figure 1. A slice of thickness $5 h^{-1}$ Mpc through the centre of the region extracted from the Millennium simulation. The image shows the dark matter distribution in the central $40 h^{-1}$ Mpc region. Void galaxies (within any void, not just the largest one) are superimposed on the dark matter distribution as blue circles. The top left and top centre panels show only the dark matter distribution and dark matter plus all galaxies in the slice, respectively. The other panels show the locations of the largest void (with dark matter particles inside the void marked green), its centre (red circle), and all void galaxies found by Brunino (top right), Colberg (second row, left column), Fairall (second row, centre), Foster (second row, right column), Gottlöber (third row, left column), Hahn/Porciani (third row, centre), Hoyle/Vogeley (third row, right column), Müller (bottom, left column), Neyrinck (bottom, centre), Pearce (bottom, right column).

Author		N_V	FF_V	δ_{DM}	N_g	δ_g	$N_{g,20}$	$\delta_{g,20}$	$(x_{max}, y_{max}, z_{max})$ [Mpc/h]	r [Mpc/h]
Brunino	P	3	0.37	-0.78	754	-0.71	7	-0.93	(38.6, 46.8, 199.5)	16.0
Colberg ¹	DM	21	0.92	-0.74	2258	-0.65	35	-0.85	(35.3, 41.2, 193.9)	29.9
Fairall	P	18	0.59	-0.73	1376	-0.67	25	-0.83	(33.0, 40.0, 200.0)	20.0
Foster/Nelson	P	3	0.41	-0.82	114	-0.96	0	-1.00	(36.3, 36.6, 192.4)	18.0
Gottlöber ²	P	9	0.35	-0.77	733	-0.70	0	-1.00	(32.1, 44.0, 192.0)	16.4
Hahn/Porciani ^{1,3}	DM	14	0.29	-0.73	248	-0.92	0	-1.00	(30.5, 33.6, 191.8)	17.2
Hoyle/Vogeley ^{1,2}	P	4	0.84	-0.68	2166	-0.56	40	-0.79	(31.9, 47.1, 193.2)	24.6
Müller ²	P	24	0.58	-0.76	1469	-0.65	0	-1.00	(30.7, 42.7, 189.1)	25.6
Neyrinck ^{1,3,4}	DM	29	0.32	-0.68	834	-0.63	14	-0.83	(30.3, 33.5, 194.9)	11.3
Pearce	DM	5	0.15	-0.90	51	-0.95	0	-1.00	(35.9, 33.8, 193.5)	11.9
Platen/Weygaert ¹	DM	167	1.0	-0.91	18	-1.00	0	-1.00	(37.5, 36.2, 194.3)	14.3
Plionis/Basilakos	DM	15	0.13	-0.92	0	-1.00	0	-1.00	(37.1, 33.8, 192.7)	10.0
Shandarin/Feldman	DM	19	0.23	-0.88	0	-1.00	0	-1.00	(31.5, 41.1, 192.7)	17.1

Table 2. An overview of some of the main results of this study: for each void finder, we give the total number of voids, N_V , in the volume considered here, the volume filling fraction, FF_V , the average dark matter overdensity, δ_{DM} , of the voids, the total number of galaxies, N_g , found in voids, the average galaxy overdensity δ_g , the number of galaxies brighter than $m_B = -20$, $N_{g,20}$, found in voids, the average galaxy overdensity using only galaxies brighter than $m_B = -20$, $\delta_{g,20}$, and positions of the centres of the largest void and their radii. We also classify the void finders into those using the dark matter (smoothed or not – DM) and those using points (galaxies or haloes – P). Notes: ¹ the voids are non-spherical, so the quoted radius is an approximation, assuming a spherical void. ² using the $B < -20$ galaxy sample. ³ the quoted centre of the void is actually the position of lowest density. ⁴ 9308 voids found; of them 2362, 525, 164, 64, 29, 13, and 5 exceed 1 through 7σ probability thresholds, respectively. We use the 5σ results for comparisons.

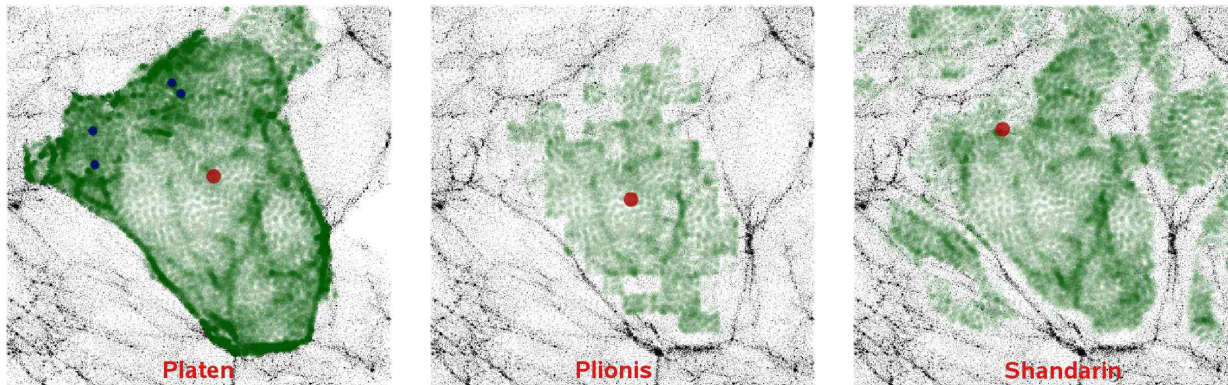


Figure 2. Same as and continued from Figure 1. Platen/Weygaert (left column), Plionis/Basilakos (centre), and Shandarin/Feldman (right column). Note that both Plionis/Basilakos and Shandarin/Feldman find no void galaxies.

4 RESULTS – COMPARISON

4.1 Basic numbers

In Table 2 we provide an overview of the results obtained with the different void finders. In particular, for each void finder, we list the total number of voids, N_V , the volume filling fraction³, FF_V , the average dark matter overdensity, δ_{DM} , of the voids, the total number of galaxies, N_g , found in voids, the corresponding average galaxy overdensity, δ_g , the number of galaxies brighter than $m_B = -20$, $N_{g,20}$, found in voids, the corresponding average galaxy overdensity using only those galaxies, $\delta_{g,20}$, and positions of the centres of the largest void and their radii.

³ The volume filling fraction is the fraction of the volume that is contained in voids, $FF_V = \sum V_i / V_{total}$, where the sum is over all voids in the sample, and V_{total} is the total volume; so, for example, $FF_V = 0.5$ means that voids fill half the volume.

When comparing these numbers it is important to keep the differences in the void finders in mind. For example, some void finders construct strictly spherical voids, whereas others build larger ones out of spherical proto-voids. In addition, there are differences in the spatial resolutions. The numbers of voids found in the volume thus can be expected to be different, and they should merely be treated as illustrative quantities.

If the different results strictly reflected the density field in the simulation, that is if all the void samples were centred on the most underdense regions and then extended out to higher density regions, there would be a simple relationship between the volume filling fraction FF_V and the average dark matter overdensity δ_{DM} . To a certain degree such a correlation does exist. For example, the *Pearce* voids are centred on the particles with the lowest local densities and are cut off at an overdensity of $\delta = -0.9$, whereas *Colberg* voids are constructed around proto-voids with $\delta = -0.8$. This results

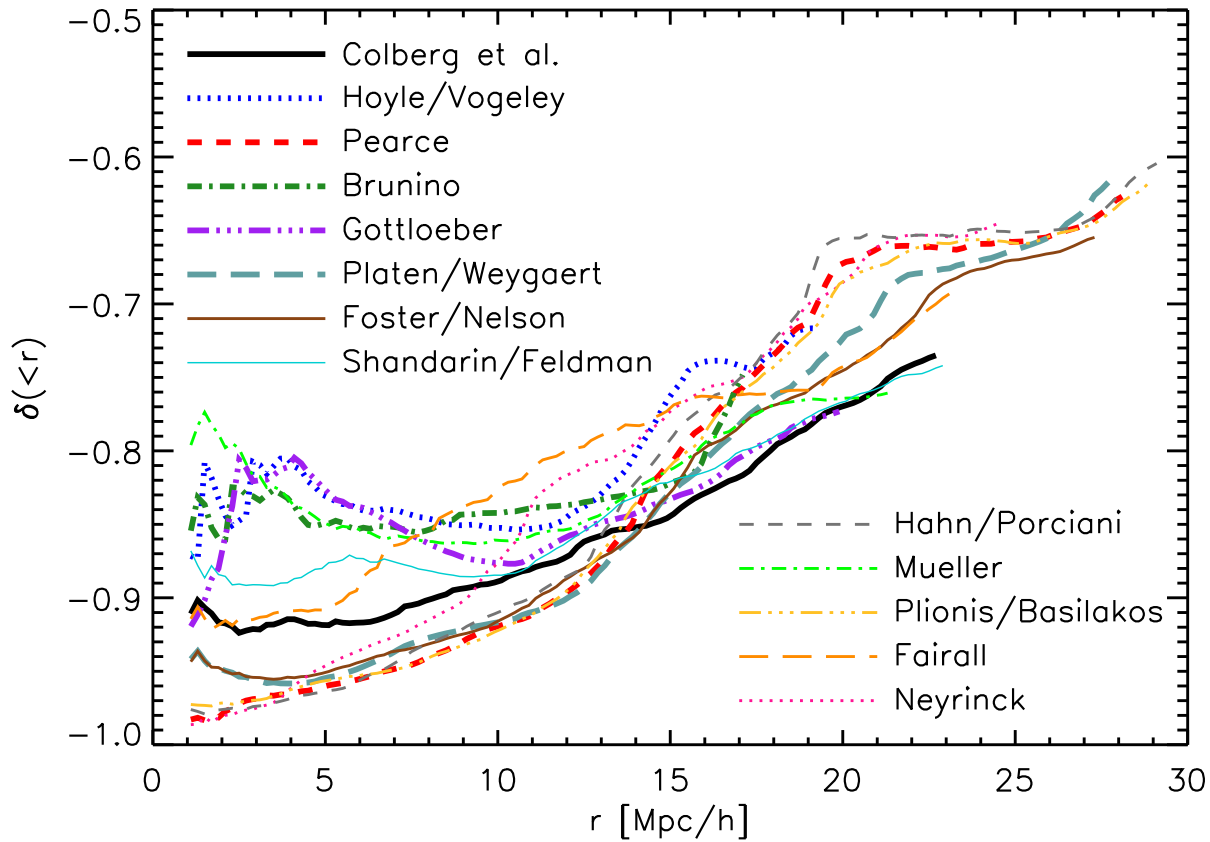


Figure 3. Radially averaged dark matter density profiles of the largest void in each of the void catalogues found by the groups involved in the study. For each void finder the profile extends out to the largest radius that can be studied, given the size of the volume. See main text for more details.

in a much lower value of FF_V for *Pearce*, whereas *Colberg’s* voids fill almost the entire volume⁴.

A more detailed examination of Table 2 reveals the key difference between the void finders we have employed: they effectively target different mean overdensities. Those which correspond to a low mean overdensity (*Pearce*, *Platen/Weygaert*, *Plionis/Basilakos* & *Shandarin*, all with $\delta \sim -0.9$) naturally contain very few galaxies as they pick out the deepest parts of the voids. At the other extreme, those finders which effectively employ higher overdensity thresholds (for instance *Colberg* and *Hoyle/Vogeley* with $\delta \sim -0.7$) pick out much larger regions and naturally enclose far more galaxies. There is nothing intrinsically wrong with different void finders targeting different overdensities, in fact in some sense pretty much the whole region could be classed as a “void”, in that it has far less dark matter than expected and consequently is depleted of galaxies. As a result secondary characteristics such as the void radius or the number density of void galaxies need to be calibrated against this effective threshold before techniques can be compared

⁴ Recall that the subvolume studied here has a mean overdensity of $\delta = -0.28$. So *Colberg’s* result is not all that surprising given the procedure it uses and the fact that the whole region is quite underdense.

in detail. Such a study is beyond the scope of this paper but should be borne in mind when examining such measures as the largest void in any particular dataset.

Given that not all void finders are density-based, there also is no direct relationship between FF_V and the number of galaxies inside the voids, N_g . There is a clear difference in N_g between the different models, with *Plionis/Basilakos* and *Shandarin/Feldman* finding no void galaxies whatsoever⁵, and the most extreme cases with several thousand void galaxies. Given the fact that the volume studied here has a mean overdensity of $\delta = -0.28$ finding lots of void galaxies is maybe not all that surprising – provided one is happy with the existence of such objects. The number of galaxies brighter than $m_B = -20$, $N_{g,20}$, is either zero or very small for all void finders. This is an important agreement for void finders which accept the existence of galaxies in voids: The overdensity of such galaxies, $\delta_{g,20}$, is smaller than about -0.8 , regardless of how voids are found.

There are also interesting agreements for quite different void finders. For example, *Plionis/Basilakos* and *Pearce* find

⁵ Note, though that for *Plionis/Basilakos* a change of the pdf fraction, below which “void cells” are considered, to the lowest 30% of the pdf, results in finding void galaxies.

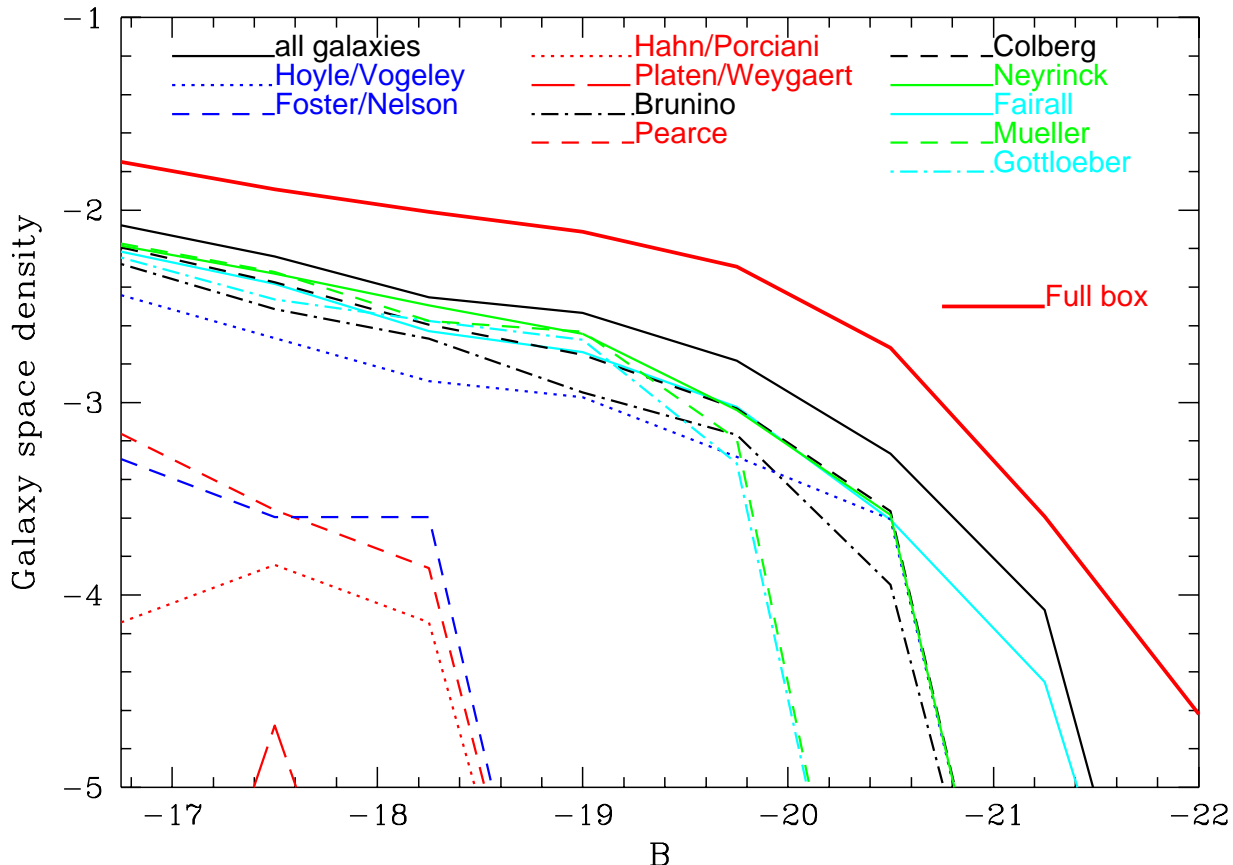


Figure 4. Space density of galaxies ($h^3/\text{Mpc}^3/\text{mag}$) as a function of dust corrected M_B for galaxies in the volume under consideration and in the catalogues of those void finders which identify galaxies inside voids. For purposes of comparison, the luminosity function of the full simulation volume is also given. Each void finder luminosity function is corrected for the volume occupied by the relevant void sample.

very similar results (FF_V , δ_{DM} , and especially the position of the largest void, but not N_g).

In Table 2, we also give the position of the centre of the largest void and its radius, as provided by the different groups. Note that some void finders build non-spherical voids, so the quoted radius merely reflects the total size of the void. While all the finders indeed locate a large void within the central region it is perhaps a little surprising that some centres are not within the central structure that is so clearly visible in the top left panel. This is in fact another consequence of the varying density thresholds employed in that those finders with effectively lower thresholds rely on larger scale structures than those that employ very low density thresholds. In addition some methods (such as those of *Brunino* and *Gottlöber*) find several voids of nearly equal size in this region, as evidenced by the number of marked blue galaxies on Figure 1 that are not within the marked green void. The key point is that the filamentary structures visible in the top left panel of Figure 1 are not very massive. Again it is clear that *void sizes depend quite strongly on how voids are found, so one has to be very careful about using void sizes to make statements about large-scale structure.*

In Figures 1 and 2, we show void galaxies found by the different groups. As noted above, the top left and top centre

panels of Figure 1 give only the dark matter distribution and the dark matter plus all model galaxies, respectively. All other panels superimpose all the recovered void galaxies on top of the dark matter distribution. In addition, for each group, we also show the largest void in green. The void centre is marked with a large red dot.

As is clearly visible, there are quite large variations between the different groups, a direct consequence of the wide variety of techniques and limits employed. Hopefully these figures shed some light on the question of what each group actually means when they refer to a “void” and illustrate the inherent difficulty of comparing results obtained using different void finders. Individually the results of each group make perfect sense, when seen in the light of how voids are identified. For example, the *Pearce* voids are some of the most underdense spheres in the volume, centred on the particles with the lowest density. Conversely, at first glance, the *Colberg* void doesn’t appear void at all and spans the entire figure, but this is a natural consequence of the very low density of the entire region.

So unless agreement has been achieved on how to define what a void really is – or should be – it is not straightforward to argue which void finder does the best job, at least when comparing images.

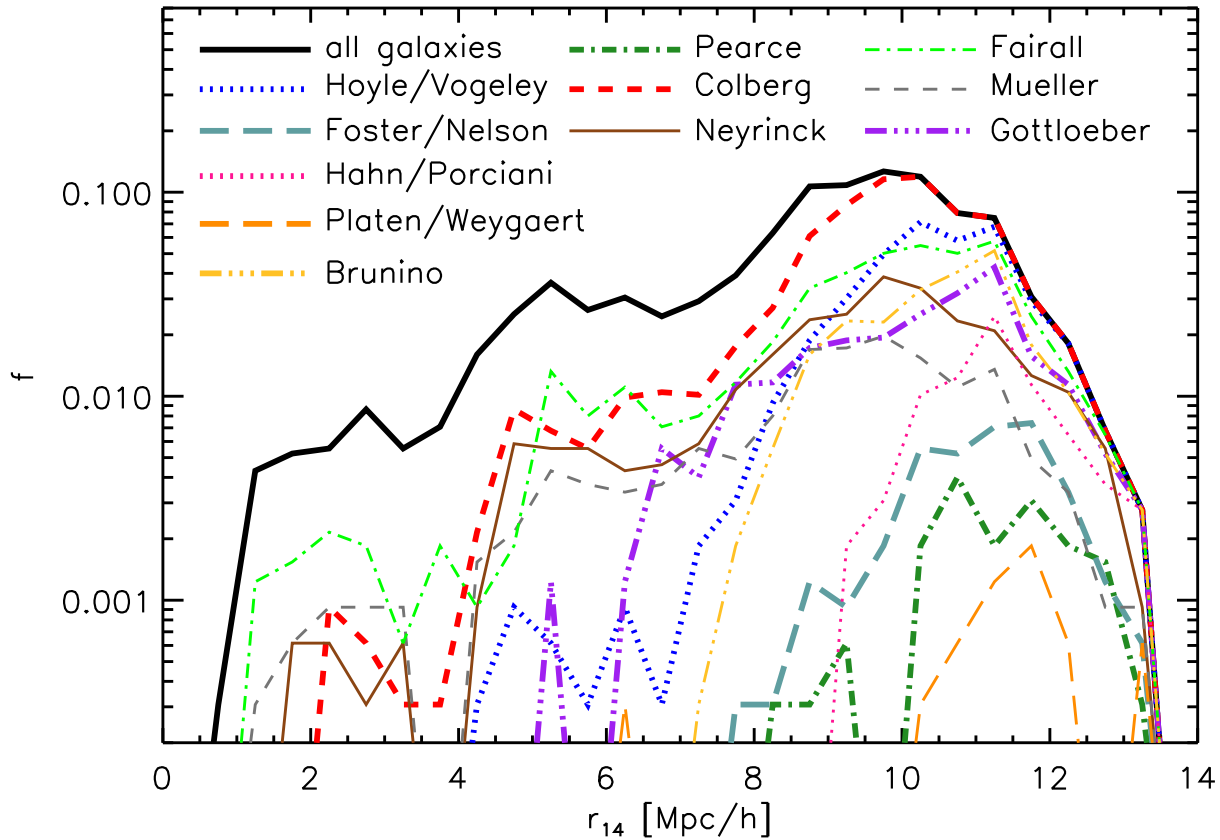


Figure 5. Distributions of the local densities of the galaxies in the results of those void finders that identify void galaxies. The local density is expressed via r_{14} , which for each galaxy gives the radius of the sphere around the galaxy that contains $10^{14} h^{-1} M_{\odot}$. For comparison purposes, the distribution of the full galaxy sample is also shown.

4.2 Void Density profiles

Despite the differences in the void-finding methods employed in earlier studies, there has been broad agreement on two facts, namely that voids are very empty in their centres and that they have very sharp edges (see, for example, Benson et al. 2003, Colberg et al. 2005, or Patiri et al. 2006b). Given the differences in the void finders, “very empty” might mean different things. It might mean that the voids are literally empty of the objects used as data – such as galaxies below some given luminosity, say – or that voids do contain some material (for example dark matter), but very little of it.

With the large variety of void finders used here, it is an interesting and important point to study the internal structure of a void. With the volume under consideration relatively small and underdense, most of the void finders find one very large void, at about the same location. We are thus limited to studying the structure of the largest void in each catalogue.

Figure 3 shows the radially averaged enclosed dark matter density as a function of radius for each of the catalogues, using the void centres given in Table 2 and shown visually on Figures 1 and 2 as a red point. It is quite important to note that such a radial average is not ideal for void finders that produce non-spherical voids. Also, for each void finder

the profile extends out to the largest radius that can be studied, given the size of the volume, so only the profiles of voids that lie close to the centre of the volume extend beyond $25 h^{-1} \text{Mpc}$. Note that these radially averaged density profiles cannot be easily compared with the average overdensities quoted in Table 2. The values quoted in Table 2 were computed using only the total void volume. However, radially averaging as in Figure 3 for voids that are not perfectly spherical will include material that does not lie inside a void.

It appears that the void finders fall into three broad categories, namely those which have central densities well below $\delta = -0.9$ (*Foster/Nelson, Hahn/Porciani, Neyrinck, Platen/Weygaert, Plionis/Basilakos, Pearce*), those with much higher, flat, central densities (*Brunino, Gottlöber, Hoyle/Vogeley, Müller*) and a third set with intermediate central densities (*Colberg, Fairall, Shandarin/Feldman*). Void finders with very low central densities all use the dark matter density field in order to identify voids in combination with a low effective overdensity threshold which restricts the size of the voids. The void finders that use (model) galaxies or haloes all have somewhat higher central densities, and much flatter central profiles. This effect is partly due to the inclusion of small haloes near the void centres as well as the difficulty of defining a void from a sparse sample of points.

Nevertheless it is clear that voids selected using the sparse tracers available from galaxies or haloes typically have central overdensities around $\delta = -0.85$ whereas those selected from the richer dark matter distribution have typically lower central density limits. Figure 3 further illustrates the role of the effective overdensity threshold driving void choice: in the central region the method of *Colberg* does not recover a particularly deep void, however, between 15 and $20h^{-1}\text{Mpc}$ this method has found the most underdense region of all the finders.

Up to a radius of around $15h^{-1}\text{Mpc}$, the largest void in each catalogue has an average density of $\delta \approx -0.85$ and at larger radii the radially averaged densities are all rising. However the entire volume studied here has a mean $\delta = -0.28$ so none of the voids runs into the very steep edges seen in earlier work as we are still well below the mean cosmic density.

Despite the differences in the central densities, we can conclude that regardless of how voids are found, their interiors are very underdense and they contain mean densities between 5% and 20% of the cosmic mean. The central regions of voids also tend to have a rather flat profile which means that regardless of how voids are found in observational surveys, follow-up work of their interiors – such as, for example, searches for hydrogen (see, for example, Giovanelli et al. 2005) – should expect very low densities of material, provided, of course, that the current model of structure formation used in the simulation is correct.

4.3 Luminosity Function

Figure 4 shows the luminosity functions of galaxies in the entire Millennium simulation (solid red line), that of the volume under consideration (solid black line) and in each of the catalogues of those void finders which identify galaxies inside voids, colour coded as shown on the figure.

We present this plot mostly for illustrative purposes, since the volume under consideration here is quite small. The key difference between the full simulation and our selected subvolume is that the galaxy formation efficiency across this entire region has been suppressed. In the full Millennium volume there are 7,151,282 galaxies with M_B between -16 and -22. If the central $40h^{-1}\text{Mpc}$ of our subvolume was a random section of the full box you would expect to find 3,661 galaxies. In practice our region has 707, or less than $\frac{1}{5}$ of the expected number. As well as this overall normalisation, compared with the full volume of the simulation, the luminosity function of the subvolume is very slightly steeper at the faint end and is deficient in bright galaxies. As mentioned before, the subvolume is underdense, so we do not expect to find many bright galaxies.

The luminosity functions of the samples that contain significant numbers of galaxies (with the exception of *Fairall*) show an even greater deficiency of bright galaxies, as evidenced earlier by the very low overdensity of bright galaxies in voids (Section 4.1). Although it is difficult to tell, it looks as if at the fainter end, the luminosity functions of the void samples all are just very slightly steeper than the subvolume one's and slightly steeper than the full simulation volume one's. This could be seen as a trend towards the most isolated galaxies being fainter than expected, as would be suggested from theoretical arguments. Those galaxies re-

siding in the most underdense regions (although there aren't very many) are certainly faint. The limit of this effect, no galaxies in the voids, is achieved by two finders, those of *Plionis/Basilakos* and *Shandarin/Feldman*.

4.4 Void galaxies and local environments

Given that we are interested in comparing results from different void finders, it is worthwhile to look at which galaxies void finders identify as belonging to a void. Apart from a galaxy's brightness, its environment, expressed through some measure of the local density, provides a useful descriptor. In order to quantify the local density, for each galaxy we compute r_{14} , the radius of the sphere that contains a mass of $10^{14}h^{-1}M_{\odot}$, roughly the mass of a small galaxy cluster.

In Figure 5, we show the distribution of the values of r_{14} , for both the complete subsample and the individual void galaxy sets. Large (small) values of r_{14} correspond to regions of low (high) density. The distribution reflects the fact that the subvolume considered here is underdense, since most galaxies reside in the low-density part of the distribution.

One would naively expect that void finders would pick up the galaxies in the lowest density regions first and then move towards the higher density regions. However, while this is true for some of the void finders, it is not true for all of them. This fact should be an important criterion for future discussions of void finders: if a void finder locates galaxies inside voids, should these be those in the most underdense environments?

Interestingly enough, the purely visual *Fairall* void-finding results in a distribution that is quite similar to *Colberg's*, and also to *Neyrinck's* and *Müller's*. Given the large differences in the methods these similarities are quite interesting, and they merit to be taken into account in future discussions of how to find voids.

5 SUMMARY AND DISCUSSION

This study represents the first systematic study of thirteen void finders, all of which have been used over the past decade to study voids, using the same data set to compare results. For the data we used real-space coordinates of particles, haloes, and semi-analytical model galaxies (Croton et al. 2005) from a subvolume of the Millennium simulation (Springel et al. 2005). The goal of this paper was *not* to argue about the best way to define or identify voids. Instead, we aimed at allowing the reader to understand the differences between the methods to allow easier comparison of studies of voids in the literature.

As outlined in Table 1, the void finders in this study range from studies of the smoothed dark matter density field to identifying empty spheres in the distribution of model galaxies, the latter either using sophisticated algorithms or simply the human eye. Given the vastly different assumption of what a void actually is, it is not surprising to see large differences between some of the void finders. However, there are also some quite encouraging agreements between methods that are quite different.

Not surprisingly, the different methods result in a large spread in basic numbers such as the number of voids, the size of the largest voids (see Table 2), or their basic appearance

(see Figures 1 and 2). We caution against putting too much emphasis on this fact. If one void finder constructs spherical voids with mean overdensities of $\delta = -0.9$ and another one builds large, irregularly shaped voids from spherical proto-voids in a distribution of galaxies, then the numbers and sizes of voids can be expected to be quite different. Likewise, the fraction of volume filled by the voids will be different. Regardless of these differences, it is quite interesting to see that the locations of the largest voids found by most of the groups agree quite well with each other. The eye finds a large void in the centre of the region studied, and the void finders do the same!

For a more detailed comparison the effective overdensity proves to be most interesting. Here, the spread is not quite as extreme as expected (see the values of δ_{DM} in Table 2), and the agreement in the overdensities of bright galaxies is quite impressive. The void finders in this study agree that there should be no or just a very small number of bright galaxies in voids. In other words, regardless of how one defines voids, there are almost no bright galaxies in them.

As Section 4.2 shows, the differences in the (radially averaged) density profiles of the largest void are also not very large, with the void centres containing only between 5% and 20% of the mean density. This means that regardless of how voids are found, their centres contain very little mass – unless, of course, our model of cosmic structure formation, which forms the basis of the simulation, is wrong. With searches for HI emission in voids under way (see Giovanelli et al. 2005 or Basilakos et al. 2007), there should soon exist additional data points, which makes it all the more pressing to move towards a more unified picture of voids.

As just mentioned, voids contain very few bright galaxies, and they contain relatively more dim galaxies, something that those void finders that identify void galaxies appear to agree on, too (see Section 4.3). Given the small number statistics in our sample, it is impossible to make stronger comments about this. What appears clear, though, is that this is an important topic to study, both observationally and theoretically, in particular since current models of galaxy formation and evolution have to account for the observed relation. For these studies to be successful, more common ground is needed as far as defining and finding voids is concerned.

We hope that this paper will trigger more detailed follow-up studies to work towards a more unified view of how to define and find voids. We believe that studies like this one, which make use of high-resolution simulations of large-scale structure, provide invaluable tools to this end, since they contain full information about the distribution of model galaxies and of the underlying density field. In the end, the model could then still be entirely wrong – a possibility that, in the light of the recent development of a standard cosmological model, appears to be somewhat unlikely – but it will still be able to provide a sound basis for calibrations of methods and ideas. This point is of particular interest since observationally (at present) only galaxies can be used to find voids. The distribution of galaxies is much harder to model, though, than the cosmic density field – the latter can be described quite well using linear theory. For studies of voids to be useful, a link needs to be forged between theory and observation. We hope that this work will provide a basis

for resolving this situation. Ultimately, as one of the most extreme cosmic environments, voids possess the potential to constrain models of galaxy formation. But for that to be the case, we need to agree on what they really are and how to find them.

ACKNOWLEDGEMENTS

This work was initiated at the Aspen Center for Physics' workshop on Cosmic Voids (June 2006) and at The Royal Netherlands Academy of Arts and Sciences Colloquium on Cosmic Voids (December 2006). We thank both institutions for their generous and valuable support of this area of research. We also thank the Virgo Supercomputing Consortium and the Lorentz Center in Leiden for their hospitality during the Winter 2007 Virgo Meeting.

The Millennium simulation used in this paper was carried out by the Virgo Supercomputing Consortium (<http://www.virgo.dur.ac.uk>) at the Computing Centre of the Max-Planck Society in Garching. We thank the Darren Croton for making the galaxy catalogue publicly available. Much of the preparation and pre-analysis required for this work was carried out at the Nottingham HPC facility.

J. Colberg is indebted to Carlos Frenk, Adrian Jenkins, and Lydia Heck for their support and help with Durham computing facilities, where part of this work was completed. C. Foster would like to thank NSERC (Canada) for support in the form of a graduate scholarship. L. Nelson would like to thank the Canada Research Chairs Program and NSERC for financial support. Figure 1 was produced using Nick Gnedin's IFRIT software (<http://home.fnal.gov/~gnedin/IFRIT>).

REFERENCES

- Arbabi-Bidgoli S., Müller V., 2002, MNRAS, 332, 205
- Basilakos S., Plionis M., Kovac K., Voglis N., 2007, MNRAS, 378, 301
- Benson A.J., Hoyle F., Torres F., Vogeley M.S., 2003, MNRAS, 340, 160
- Beucher S., Lantuejoul C., 1979, Proceedings International Workshop on Image Processing, CCETT/IRISA, Rennes, France
- Beucher S., Meyer F., 1993, Mathematical Morphology in Image Processing, eds. M. Dekker, New York, Ch. 12, pp. 433-481
- Blumenthal G.R., da Costa L.N., Goldwirth D.S., Lecar M., Piran T., 1992, ApJ, 388, 234
- Bolejko K., Krasinski A., Hellaby C., 2005, MNRAS, 362, 213
- Brunino R., Trujillo R., Pearce F.R., Thomas P.A., 2007, MNRAS, 375, 184
- Ceccarelli L., Padilla N.D., Valotto C., Lambas D.G., 2006, MNRAS, 373, 1440
- Colberg J.M., Sheth R.K., Diaferio A., Gao L., Yoshida N., 2005, MNRAS, 360, 216
- Colless M., et al. (the 2dFGRS Team), 2001, MNRAS, 328, 1039
- Croton D.J., et al., 2004, MNRAS, 352, 828
- Croton D.J., et al., 2005, MNRAS, 365, 11
- de Lapparent, V., Geller M.J., Huchra J.P., 1986, ApJ, 302, 1
- Dubinski J., da Costa L.N., Goldwirth D.S., Lecar M., Piran T., 1993, ApJ, 410, 458
- El-Ad H., Piran T., Costa L.N., 1997, MNRAS, 287, 790
- El-Ad H., Piran T., 1997, ApJ, 491, 421
- Foster, C., Nelson, L., submitted ApJ

- Furlanetto S.R., Piran T., 2006, MNRAS, 366, 467
- Giovanelli R. et al., 2005, AJ, 130, 2598
- Goldberg D.M., Vogeley M.S., 2004, ApJ, 605, 1
- Goldberg D.M., Jones T.D., Hoyle F., Rojas R.R., Vogeley M.S., Blanton M.R., 2005, ApJ, 621, 643
- Gottlöber S., Lokas E.L., Klypin A., Hoffman Y., 2003, MNRAS, 344, 715
- Hahn O., Porciani C., Carollo C. M., Dekel A., MNRAS, 375, 489
- Hoefl M., Yepes G., Gottlöber S., Springel V., 2006, 371, 401
- Hoyle F., Vogeley M.S., 2002, ApJ, 566, 641
- Hoyle F., Vogeley M.S., 2004, ApJ, 607, 751
- Hoyle F., Rojas R.R., Vogeley M.S., Brinkman J., 2005, ApJ, 620, 618
- Kauffmann, G., Fairall, A, 1991, MNRAS, 248, 313
- Kirshner R.P., Oemler A., Schechter P.L., Shectman S.A., 1981, ApJ, 248, L57
- Lee J., Park D., 2006, ApJ, 652, 1
- Mathis H., White S.D.M., 2002, MNRAS, 337, 1193
- Monaghan J.J., Lattanzio, J.C., 1985, A&A, 149, 135
- Müller V., Arbabi-Bidgoli S., Einasto J., Tucker D., 2000, MNRAS, 318, 280
- Neyrinck M.C., Gnedin N.Y., Hamilton A.J.S., 2005, MNRAS, 356, 1222
- Neyrinck M.C., 2008, MNRAS, in press (arXiv:0712.3049)
- Padilla N.D., Ceccarelli L., Lambas D.G., 2005, MNRAS, 363, 977
- Park D., Lee J., 2007, PhRvL, 98, 1301
- Patiri S.G., Betancourt-Rijo J.E., Prada F., Klypin A., Gottlöber S., 2006a, MNRAS, 369, 335
- Patiri S.G., Prada F., Holtzman J., Klypin A., Betancourt-Rijo J.E., 2006b, MNRAS, 372, 1710
- Patiri S.G., Betancourt-Rijo J.E., Prada F., 2006c, MNRAS, 368, 1132
- Pelupessy F.I., Schaap W.E., Van de Weygaert R., 2003, A&A, 403, 389
- Peebles P.J.E., 2001, ApJ, 557, 495
- Platen E., 2005, *Segmenting the Universe*, master's thesis, University of Groningen
- Platen E., Van de Weygaert R., Jones B.J.T., 2007, MNRAS, 380, 551
- Plionis M., Basilakos S., 2002, MNRAS, 330, 399
- Regos E., Geller M.J., 1991, ApJ, 377, 14
- Rojas R.R., Vogeley M.S., Hoyle F., Brinkman J., 2004, ApJ, 617, 50
- Rojas R.R., Vogeley M.S., Hoyle F., Brinkman J., 2005, ApJ, 624, 571
- Schaap, W.E., van de Weygaert, R., 2000, A&A, 363, L29
- Schaap, W.E., 2007, *the Delaunay Tessellation Field Estimator*, Ph.D. thesis, University of Groningen
- Shandarin S.F., Sheth J., Sahni V., 2004, MNRAS, 353, 162
- Shandarin S.F., Feldman H.A., Heitmann K., Habib S., 2006, MNRAS, 367, 1629
- Sheth R.K., Van de Weygaert R., 2004, MNRAS, 350, 517
- Springel V., et al. (Virgo Consortium), 2005, Nature, 435, 629
- Tinker J.L., Weinberg D.H., Warren M.S., 2006, ApJ, 647, 737
- Tikhonov A.V., 2007, AstL, 33, 499
- Trujillo I., Carretero C., Patiri S.G., 2006, ApJ, 640, 111
- von Benda-Beckmann A. M., Müller V., 2008, MNRAS, 65
- Van de Weygaert R., Van Kampen E., 1993, MNRAS, 263, 481
- York D.G., et al. (the SDSS Collaboration), 2000, AJ, 120, 1579